Scientific Research Publishing

Journal of Applied Mathematics and Physics, 2022, 10, 3369-3384
https://www.scirp.org/journal/jamp
ISSN Online: 2327-4379
ISSN Print: 2327-4352

Dislocations in Cosserat Plates

Roman Kvasov[1*], Lev Steinberg[2]

[1]Department of Mathematics, University of Puerto Rico at Aguadilla, Puerto Rico, USA
[2]Department of Mathematics, University of Puerto Rico at Mayaguez, Puerto Rico, USA
Email: *roman.kvasov@upr.edu

How to cite this paper: Kvasov, R. and Steinberg, L. (2022) Dislocations in Cosserat Plates. *Journal of Applied Mathematics and Physics*, **10**, 3369-3384.
https://doi.org/10.4236/jamp.2022.1011223

Received: October 8, 2022
Accepted: November 26, 2022
Published: November 29, 2022

Copyright © 2022 by author(s) and Scientific Research Publishing Inc.
This work is licensed under the Creative Commons Attribution International License (CC BY 4.0).
http://creativecommons.org/licenses/by/4.0/

Open Access

Abstract

This article provides the numerical modeling of the dislocations in the Cosserat elastic plates based on the Cosserat Plates Theory developed by the authors. The dislocation is modeled by a sequence of domains that converge to the point of the dislocation and by a residual force distributed around that point. The plate deformation caused by the dislocation is calculated using the Finite Element Method. We also discuss the effect of the dislocation on the cavities present in the Cosserat plates.

Keywords

Dislocation, Cosserat Plates, Cosserat Materials

1. Introduction

In the Classical Elasticity, the movement of the particles within the elastic body is described by the displacement vector. Since there are no particle rotations considered, each particle has only three degrees of freedom. The surface loads are described by the force vector, which implies the symmetry of the corresponding stress tensor.

It has been noted that such materials as foams, composites, concrete and human bones represent materials with microstructure and cannot always be described by the Classical Elasticity [1] [2] [3] [4] [5] [6].

The theory that takes into account the size effect of the particles and their rotations is Cosserat Elasticity. It employs three additional degrees of freedom for material particles, which represent their microrotations. The description of the surface loads is done by the force and moment vectors. The stress tensor is asymmetric and an additional couple stress tensor is incorporated. A total of six elastic constants are needed for the correct description of the Cosserat solid.

The Theory of Cosserat Elasticity starts with a pioneering work published by

Eugene and Francois Cosserat at the beginning of the 20th century [7]. Since the 1960s, the number of publications on Cosserat Elasticity started to grow and has not stopped since. The complete theory of three-dimensional asymmetric elasticity gave rise to a variety of Cosserat plate theories. Naghdi obtained the linear theory of Cosserat plate [8] and Eringen proposed a complete theory of plates in the framework of Cosserat Elasticity [9]. Steinberg proposed to use the Reissner plate theory as a basis for the theory of Cosserat plates in [10]. The finite element modeling for this theory is provided in [11].

The first version of the Cosserat Plate Theory, presented by the authors in [12], includes some additional assumptions leading to the introduction of the splitting parameter. This parametric theory produces the equilibrium equations, constitutive relations, and the optimal value of the minimization of the elastic energy of the Cosserat plate. The paper [12] also provides the analytical solutions of the presented plate theory and the three-dimensional Cosserat elasticity for simply supported rectangular plates. The comparison of these solutions showed that the precision of the developed Cosserat plate theory is similar to the precision of the classical plate theory developed by Reissner [13] [14].

The numerical modeling of the bending of simply supported rectangular plates is given in [15]. Here the Cosserat plate field equations and the exact formula for the optimal value of the splitting parameter were developed. The solution of the Cosserat plate was shown to converge to the Reissner plate as the Cosserat elasticity parameters tend to zero. The Cosserat plate theory showed the agreement with the size effect, confirming that the plates of smaller thickness are more rigid than is expected from the Reissner model.

The extension of the static model of Cosserat elastic plates to the dynamic problems is presented in [16]. The computations predict a new kind of natural frequencies associated with the material microstructure and were shown to be compatible with the size effect principle reported in [15] for the Cosserat plate bending.

The numerical study of Cosserat elastic plate deformation based on the parametric theory of Cosserat plates using the Finite Element Method is presented in [17]. The paper discusses the existence and uniqueness of the weak solution, convergence of the proposed FEM and its numerical validation by estimating the order of convergence. The Finite Element analysis of clamped Cosserat plates of different shapes under different loads is also provided. The numerical analysis of plates with circular holes shows that the stress concentration factor around the hole is less than the classical value, and smaller holes exhibit less stress concentration as would be expected on the basis of the classical elasticity.

The Dynamics of Cosserat Plates of different shapes and orientations of micro-elements are given in the chapter [18]. The numerical computations of the plate free vibrations showed the existence of the additional frequencies that depend on the orientation of microelements. The comparison of the eigenvalue frequencies with the three-dimensional Cosserat Elastodynamics shows a high agreement with the exact values.

The complete Cosserat Plate Theory has been recently published in the book [19]. The text presents the classification of the Cosserat plates, the foundation and the validation of the Cosserat Plate Theory, the exact solutions for statics and dynamics, and the Finite Element computations. We also discuss such unique properties of the Cosserat plates as plate stiffness, stress concentration, plate resonances and dynamic anisotropy.

Linearly elastic bodies with defects in the form of dislocations are studied in [20], where a two-dimensional problem is considered on the basis of the three-dimensional Classical Elasticity ignoring the microstructure of the material. The gauge theory of dislocations and disclinations is developed in [21]. The convection flow of unsteady Maxwell fluid in the course of a porous plate is investigated in [22]. Dislocations and their effects are studied at the level of quantum mechanics in [23].

The current article provides the modeling of the dislocations in Cosserat plates, *i.e.* two-dimensional structural elements made of materials with microstructure. Our approach is based on the continuum mechanics where quantum effects are not considered. In this article the dislocations are studied in the framework of Cosserat Elasticity in contrast to [20] that is based on Classical Elasticity, ignoring the influence of microstructure and rotational effects of the microelements. The numerical results of the deformation caused by the dislocation are based on the Finite Element algorithm developed in [17]. The Finite Element provides the accurate approximations of the kinematic variables, stresses, couples, strains and torsions for Cosserat plates of arbitrary shapes (including the plates with holes). The possible effect of the dislocation on a hole incorporated into the Cosserat plate is discussed as well.

2. Cosserat Plate Theory

We study the deformation of the Cosserat body without body forces and body moments. The corresponding Cosserat equilibrium equations are given as in [15]:

$$\sigma_{ji,j} = 0, \tag{1}$$

$$\varepsilon_{ijk}\sigma_{jk} + \mu_{ji,j} = 0, \tag{2}$$

where the σ_{ji} is the stress tensor, μ_{ji} is the couple stress tensor, ε_{ijk} and is the Levi-Civita tensor.

The constitutive formulas for the Cosserat material are given in the following form [19]:

$$\sigma_{ji} = (\mu+\alpha)\gamma_{ji} + (\mu-\alpha)\gamma_{ij} + \lambda\gamma_{kk}\delta_{ij}, \tag{3}$$

$$\mu_{ji} = (\gamma+\varepsilon)\chi_{ji} + (\gamma-\varepsilon)\chi_{ij} + \beta\chi_{kk}\delta_{ij}, \tag{4}$$

where μ, λ are the Lamé parameters and α, β, γ, ε are the Cosserat elasticity parameters.

The strain-displacement and torsion-microrotation relations are given as in [19]:

$$\gamma_{ji} = u_{i,j} + \varepsilon_{ijk}\phi_k, \tag{5}$$

$$\chi_{ji} = \phi_{i,j}, \tag{6}$$

where u_i and ϕ_i represent the displacement vector and the rotation vector respectfully.

We consider the Cosserat plate P of thickness h and $x_3 = 0$ representing its middle plane. The top and bottom surfaces of the plate are contained in the planes $x_3 = h/2$ and $x_3 = -h/2$ respectively. In the Cosserat Plate Theory we assume that the variation of the components of the stressses σ_{ji}, couple stresses μ_{ji}, displacements u_i and rotations ϕ_i are represented by the polynomials of the variable x_3 in such way that it is consistent with the equilibrium Equations (1)-(2), constitutive formulas (3)-(4) and the strain-displacement relation (5) and torsion-microrotation relation (6). Here we will provide the summary of the Cosserat Plate assumptions given in [19]:

$$\sigma_{\alpha\beta} = m_{\alpha\beta}(x_1, x_2)\zeta$$

$$\sigma_{3\beta} = q_\beta(x_1, x_2)\left(1-\zeta^2\right)$$

$$\sigma_{\alpha 3} = q^*_\alpha(x_1, x_2)\left(1-\zeta^2\right) + \hat{q}_\alpha(x_1, x_2)$$

$$\sigma_{33} = \frac{3}{4}\left(\zeta - \frac{\zeta^3}{3}\right)p^*(x_1, x_2) + \frac{1}{2}\hat{p}(x_1, x_2)\zeta + \sigma_0(x_1, x_2)$$

$$\mu_{\alpha\beta} = r^*_{\alpha\beta}(x_1, x_2)\left(1-\zeta^2\right) + \hat{r}_{\alpha\beta}(x_1, x_2)$$

$$\mu_{\alpha 3} = s_\alpha(x_1, x_2)\zeta$$

$$\mu_{3\beta} = 0$$

$$\mu_{33} = 0$$

$$u_\alpha = \psi_\alpha(x_1, x_2)\zeta$$

$$u_3 = w^*(x_1, x_2)\left(1-\zeta^2\right) + \hat{w}(x_1, x_2)$$

$$\phi_\alpha = \omega^*_\alpha(x_1, x_2)\left(1-\zeta^2\right) + \hat{\omega}_\alpha(x_1, x_2)$$

$$\phi_3 = \omega_3(x_1, x_2)\zeta$$

where

$$p^*(x_1, x_2) = \eta\, p(x_1, x_2), \tag{7}$$

$$\hat{p}(x_1, x_2) = (1-\eta)\, p(x_1, x_2), \tag{8}$$

and η is called the splitting parameter.

The substitution of the stress assumptions into the three-dimensional Cosserat equilibrium Equations (1)-(2) results in the following equilibrium system of equations for Cosserat Plate [19]:

$$M_{\alpha\beta,\alpha} - Q_\beta = 0, \tag{9}$$

$$Q^*_{\alpha,\alpha} + p^* = 0, \tag{10}$$

$$\hat{Q}_{\alpha,\alpha} + \hat{p} = 0, \tag{11}$$

$$R^*_{\alpha\beta,\alpha} + \varepsilon_{3\beta\gamma}\left(Q^*_\gamma - Q_\gamma\right) = 0, \tag{12}$$

$$\hat{R}_{\alpha\beta,\alpha} + \varepsilon_{3\beta\gamma}\hat{Q}_\gamma = 0, \tag{13}$$

$$S_{\alpha,\alpha} + \varepsilon_{3\beta\gamma}M_{\beta\gamma} = 0. \tag{14}$$

Here

M_{11}, M_{22} —bending moments,

M_{12}, M_{21} —twisting moments,

Q_α —shear forces,

$Q^*_\alpha, \hat{Q}_\alpha$ —transverse shear forces,

$R^*_{11}, R^*_{22}, \hat{R}_{11}, \hat{R}_{22}$ —Cosserat bending moments,

$R^*_{12}, R^*_{21}, \hat{R}_{12}, \hat{R}_{21}$ —Cosserat twisting moments,

S_α —Cosserat couple moments,

are related to the Cosserat plate assumptions as follows:

$$M_{\alpha\beta} = \frac{h^2}{6}m_{\alpha\beta},$$

$$Q_\alpha = \frac{2h}{3}q_\alpha,$$

$$Q^*_\alpha = \frac{2h}{3}q^*_\alpha,$$

$$\hat{Q}_\alpha = \frac{2h}{3}\hat{q}_\alpha,$$

$$R^*_{\alpha\beta} = \frac{2h}{3}r^*_{\alpha\beta},$$

$$\hat{R}_{\alpha\beta} = \frac{2h}{3}\hat{r}_{\alpha\beta},$$

$$S_\alpha = \frac{h^2}{6}s_\alpha.$$

The constitutive formulas for the Cosserat Plate are given as in [19]:

$$M_{\alpha\alpha} = \frac{h^3\mu(\lambda+\mu)}{3(\lambda+2\mu)}\Psi_{\alpha,\alpha} + \frac{\lambda\mu h^3}{6(\lambda+2\mu)}\Psi_{\beta,\beta} + \frac{\left(6p^* + 5\hat{p}\right)\lambda h^2}{60(\lambda+2\mu)}, \tag{15}$$

$$M_{\beta\alpha} = \frac{(\mu-\alpha)h^3}{12}\Psi_{\alpha,\beta} + \frac{h^3(\alpha+\mu)}{12}\Psi_{\beta,\alpha} + (-1)^\beta\frac{\alpha h^3}{6}\Omega_3, \tag{16}$$

$$\begin{aligned} Q_\alpha = {} & \frac{5h(\alpha+\mu)}{6}\Psi_\alpha + \frac{5(\mu-\alpha)h}{6}\hat{W}_{,\alpha} + \frac{5(\mu-\alpha)h}{6}W^*_{,\alpha} \\ & + (-1)^\beta\frac{5h\alpha}{3}\Omega^*_\beta + (-1)^\beta\frac{5h\alpha}{3}\hat{\Omega}_\beta, \end{aligned} \tag{17}$$

$$\begin{aligned} Q^*_\alpha = {} & \frac{5(\mu-\alpha)h}{6}\Psi_\alpha + \frac{5(\mu-\alpha)^2 h}{6(\mu+\alpha)}\hat{W}_{,\alpha} + \frac{5(\mu+\alpha)h}{6}W^*_{,\alpha} \\ & + (-1)^\alpha\frac{5h\alpha}{3}\Omega^*_\beta + (-1)^\alpha\frac{5h\alpha(\mu-\alpha)}{3(\mu+\alpha)}\hat{\Omega}_\beta, \end{aligned} \tag{18}$$

$$\hat{Q}_\alpha = \frac{8\alpha\mu h}{3(\mu+\alpha)}\hat{W}_{,\alpha} + (-1)^\alpha \frac{8\alpha\mu h}{3(\mu+\alpha)}\hat{\Omega}_\beta, \tag{19}$$

$$R^*_{\alpha\alpha} = \frac{10h\gamma(\beta+\gamma)}{3(\beta+2\gamma)}\Omega^*_{\alpha,\alpha} + \frac{5h\beta\gamma}{3(\beta+2\gamma)}\Omega^*_{\beta,\beta}, \tag{20}$$

$$R^*_{\beta\alpha} = \frac{5(\gamma-\varepsilon)h}{6}\Omega^*_{\beta,\alpha} + \frac{5h(\gamma+\varepsilon)}{6}\Omega^*_{\alpha,\beta}, \tag{21}$$

$$\hat{R}_{\alpha\alpha} = \frac{8\gamma(\gamma+\beta)h}{3(\beta+2\gamma)}\hat{\Omega}_{\alpha,\alpha} + \frac{4\gamma\beta h}{3(\beta+2\gamma)}\hat{\Omega}_{\beta,\beta}, \tag{22}$$

$$\hat{R}_{\beta\alpha} = \frac{2(\gamma-\varepsilon)h}{3}\hat{\Omega}_{\beta,\alpha} + \frac{2(\gamma+\varepsilon)h}{3}\hat{\Omega}_{\alpha,\beta}, \tag{23}$$

$$S_\alpha = \frac{\gamma\varepsilon h^3}{3(\gamma+\varepsilon)}\Omega_{3,\alpha}. \tag{24}$$

Here

Ψ_1 —rotation of the middle plane around x_1 axis,

Ψ_2 —rotation of the middle plane around x_2 axis,

$W^* + \hat{W}$ —vertical deflection of the middle plate,

$\Omega_1^* + \hat{\Omega}_1$ —microrotations in the middle plane around x_1 axis,

$\Omega_2^* + \hat{\Omega}_2$ —microrotations in the middle plane around x_2 axis,

Ω_3 —rate of change of the microrotation ϕ_3 along x_3

are related to the Cosserat plate assumptions as follows:

$$\Psi_\alpha = \frac{2}{h}\psi_\alpha(x_1, x_2),$$

$$W^* = \frac{4}{5}w^*(x_1, x_2),$$

$$\hat{W} = \hat{w}(x_1, x_2),$$

$$\Omega^*_\alpha = \frac{4}{5}\omega^*_\alpha(x_1, x_2),$$

$$\hat{\Omega}_\alpha = \hat{\omega}_\alpha(x_1, x_2),$$

$$\Omega_3 = \frac{2}{h}\omega_3(x_1, x_2),$$

The Cosserat plate field equations are obtained by substituting the constitutive formulas (15)-(24) into the bending system of Equations (9)-(14). If the solution vector v of the kinematic variables is defined as

$$v = \left[\Psi_1, \Psi_2, W, \Omega_3, \Omega_1, \Omega_2, W^*, \hat{\Omega}_1, \hat{\Omega}_2\right]^{\mathrm{T}}, \tag{25}$$

then the Cosserat plate bending field equations can be written in the following form

$$Lv = f(\eta). \tag{26}$$

The operator L here is given as

$$\begin{bmatrix} L_{11} & L_{12} & L_{13} & L_{14} & 0 & L_{16} & 0 & L_{18} & L_{19} \\ L_{12} & L_{22} & L_{23} & L_{24} & L_{25} & 0 & L_{27} & 0 & L_{29} \\ L_{31} & L_{32} & L_{33} & L_{34} & L_{35} & L_{36} & L_{37} & L_{38} & 0 \\ L_{41} & L_{42} & L_{43} & L_{44} & L_{45} & L_{46} & L_{47} & L_{48} & 0 \\ 0 & L_{52} & L_{53} & L_{54} & L_{55} & L_{56} & L_{57} & 0 & 0 \\ L_{61} & 0 & L_{63} & L_{64} & L_{65} & L_{66} & 0 & L_{68} & 0 \\ 0 & 0 & 0 & L_{74} & 0 & 0 & L_{77} & L_{78} & 0 \\ 0 & 0 & 0 & L_{84} & 0 & 0 & L_{87} & L_{88} & 0 \\ L_{91} & L_{92} & 0 & 0 & 0 & 0 & 0 & 0 & L_{99} \end{bmatrix}$$

and the right-hand side $f(\eta)$ vector is

$$f(\eta) = \begin{bmatrix} -\dfrac{h^3\lambda\left(6p_{,1}^* + 5\hat{p}_{,1}\right)}{120\left(\lambda+2\mu\right)} \\ -\dfrac{h^3\lambda\left(6p_{,2}^* + 5\hat{p}_{,2}\right)}{120\left(\lambda+2\mu\right)} \\ -\dfrac{6p^* + 5\hat{p}}{6} \\ -p^* \\ 0 \\ 0 \\ 0 \\ 0 \\ 0 \end{bmatrix},$$

The operators L_{ij} are defined as follows:

$$L_{11} = c_1\frac{\partial^2}{\partial x_1^2} + c_2\frac{\partial^2}{\partial x_2^2} - c_3,\ L_{12} = c_4\frac{\partial^2}{\partial x_1 x_2},$$

$$L_{13} = c_5\frac{\partial}{\partial x_1},\ L_{14} = c_5\frac{\partial}{\partial x_1},$$

$$L_{16} = c_6,\ L_{18} = c_6,$$

$$L_{19} = c_7\frac{\partial}{\partial x_2},\ L_{21} = c_4\frac{\partial^2}{\partial x_1 x_2},$$

$$L_{22} = c_2\frac{\partial^2}{\partial x_1^2} + c_1\frac{\partial^2}{\partial x_2^2} - c_3,\ L_{23} = c_5\frac{\partial}{\partial x_2},$$

$$L_{24} = c_5\frac{\partial}{\partial x_2},\ L_{25} = -c_6,$$

$$L_{27} = -c_6,\ L_{29} = -c_7\frac{\partial}{\partial x_1},$$

$$L_{31} = c_5\frac{\partial}{\partial x_1},\ L_{32} = -c_5\frac{\partial}{\partial x_1},$$

$$L_{33} = c_3\frac{\partial^2}{\partial x_1^2} + c_3\frac{\partial^2}{\partial x_2^2},\ L_{34} = c_3\frac{\partial^2}{\partial x_1^2} + c_3\frac{\partial^2}{\partial x_2^2},$$

$$L_{35} = -c_6 \frac{\partial}{\partial x_2},\ L_{36} = c_6 \frac{\partial}{\partial x_1},$$

$$L_{37} = -c_6 \frac{\partial}{\partial x_2},\ L_{38} = c_6 \frac{\partial}{\partial x_1},$$

$$L_{41} = c_5 \frac{\partial}{\partial x_1},\ L_{42} = -c_5 \frac{\partial}{\partial x_1},$$

$$L_{43} = c_3 \frac{\partial^2}{\partial x_1^2} + c_3 \frac{\partial^2}{\partial x_2^2},\ L_{44} = c_8 \frac{\partial^2}{\partial x_1^2} + c_8 \frac{\partial^2}{\partial x_2^2},$$

$$L_{45} = -c_6 \frac{\partial}{\partial x_2},\ L_{46} = c_6 \frac{\partial}{\partial x_1},$$

$$L_{47} = -c_9 \frac{\partial}{\partial x_2},\ L_{48} = c_9 \frac{\partial}{\partial x_1},$$

$$L_{52} = -c_6,\ L_{53} = c_6 \frac{\partial}{\partial x_2},$$

$$L_{54} = c_9 \frac{\partial}{\partial x_2},\ L_{55} = c_{10} \frac{\partial^2}{\partial x_1^2} + c_{11} \frac{\partial^2}{\partial x_2^2} - 2c_6,$$

$$L_{56} = c_{12} \frac{\partial^2}{\partial x_1 x_2},\ L_{57} = -c_{13},$$

$$L_{61} = c_6,\ L_{63} = -c_6 \frac{\partial}{\partial x_2},$$

$$L_{64} = -c_9 \frac{\partial}{\partial x_2},\ L_{65} = c_{12} \frac{\partial^2}{\partial x_1 x_2},$$

$$L_{66} = c_{10} \frac{\partial^2}{\partial x_1^2} + c_{11} \frac{\partial^2}{\partial x_2^2} - 2c_6,\ L_{67} = -c_{13},$$

$$L_{74} = c_{14} \frac{\partial}{\partial x_2},\ L_{77} = c_{10} \frac{\partial^2}{\partial x_1^2} + c_{11} \frac{\partial^2}{\partial x_2^2} - c_{14},$$

$$L_{78} = c_{12} \frac{\partial^2}{\partial x_1 x_2},\ L_{84} = c_{14} \frac{\partial}{\partial x_2},$$

$$L_{78} = c_{12} \frac{\partial^2}{\partial x_1 x_2},\ L_{88} = c_{11} \frac{\partial^2}{\partial x_1^2} + c_{10} \frac{\partial^2}{\partial x_2^2} - c_{14},$$

$$L_{91} = -c_7 \frac{\partial}{\partial x_2},\ L_{92} = c_7 \frac{\partial}{\partial x_1},$$

$$L_{99} = c_{15} \frac{\partial^2}{\partial x_1^2} + c_{15} \frac{\partial^2}{\partial x_2^2} - 2c_7,$$

where c_i are the constants given as

$$c_1 = \frac{h^4 \mu(\lambda+\mu)}{6(\lambda+2\mu)},\ c_2 = \frac{h^4(\alpha+\mu)}{24},$$

$$c_3 = \frac{5h(\alpha+\mu)}{6},\ c_4 = \frac{h^4\left(\mu(3\lambda+2\mu) - \alpha(\lambda+2\mu)\right)}{24(\lambda+2\mu)},$$

$$c_5 = \frac{5h(\alpha-\mu)}{6},\ c_6 = \frac{5h\alpha}{3},$$

$$c_7 = \frac{h^4\alpha}{12},\ c_8 = \frac{5h(\alpha-\mu)^2}{6(\alpha+\mu)},$$

$$c_9 = \frac{5h\alpha(\alpha-\mu)}{3(\alpha+\mu)},\ c_{10} = \frac{10h\gamma(\beta+\gamma)}{3(\beta+2\gamma)},$$

$$c_{11} = \frac{5h(\gamma+\varepsilon)}{6},\ c_{12} = \frac{5h(2\gamma(\gamma-\varepsilon)+\beta(3\gamma-\varepsilon))}{6(\beta+2\gamma)},$$

$$c_{13} = \frac{10h\alpha^2}{3(\alpha+\mu)},\ c_{14} = \frac{10h\alpha\mu}{3(\alpha+\mu)},$$

$$c_{15} = \frac{h^4\gamma\varepsilon}{6(\gamma+\varepsilon)}.$$

The system of equations (26) is an elliptic parametric system of nine partial differential equations. The exact solutions of this system for rectangular plates are given in [15] and the numerical solutions for the plates of arbitrary shapes are given in [17].

3. Numerical Results

The appearance of defects, cracks, dislocations or other inhomogeneities can affect the performance of the material. It creates a stress field around the dislocation and might affect the body as a whole and also act on its cavities and displace them. Therefore, correctly assessing the effect of the dislocation is essential for use of the material in applications.

For the numerical modeling we will consider a Cosserat plate with a dislocation (inclusion, defect, inhomogeneity) and follow [20].

Let b_i be the Burger's vector, denoting an additional displacement of the lattice points. The distortion tensor is

$$w_{ik} = u_{k,i}$$

and

$$\oint_L w_{ik}\,\mathrm{d}x_i = -b_k$$

or equivalently

$$\int_{S_L} e_{ilm} w_{mk,j}\,\mathrm{d}f_i = -b_k$$

The two-dimensional delta-function $\delta(\xi)$ satisfies

$$\int \delta(\xi)\tau\cdot\mathrm{d}\mathbf{f} = \tau_i \int_{S_L} \delta(\xi)\cdot\mathrm{d}f_i = 1$$

Therefore

$$e_{ilm} w_{mk,j}\,\mathrm{d}f_i = -\tau_i b_k \delta(\xi)$$

Let (a,b) be the position of the dislocation. We will simulate the effect of

the two-dimensional delta function $\delta(\xi)$ by assuming the boundary condition on some circular neighborhood represented by the function $g(x_1, x_2)$:

$$g(x_1, x_2) = \frac{1}{2\pi}\arctan\left(\frac{x_2 - b}{x_1 - a}\right) \tag{27}$$

The function $g(x_1, x_2)$ gives a constant for any line integral along the circle $L^{(r)}$ of radius r centered at the dislocation:

$$\oint_{L^{(r)}} g_{,i}\mathrm{d}x_i = 1$$

Let us define

$$J_j = \int_S k_{ij} n_i \mathrm{d}A$$

where k_{ij} is the material stress tensor.

The values of J_j can be found from [20]:

$$J_1 = \int_0^{2\pi} \sigma_{\phi\phi}(\phi)\cos\phi \mathrm{d}\phi$$

$$J_2 = \int_0^{2\pi} \sigma_{\phi\phi}(\phi)\sin\phi \mathrm{d}\phi$$

where

$$\sigma_{\phi\phi}(\phi) = \sigma_{11}^C + \sigma_{22}^C + 2\left(\sigma_{\phi\phi}^L(r,\phi) - \sigma_{rr}^L(r,\phi)\right)$$

$\sigma_{\phi\phi}(\phi)$ is the hoop stress, σ_{11}^C, σ_{22}^C are the stresses in Cartesian coordinates at the center of the hole, $\sigma_{\phi\phi}^L(r,\phi)$, $\sigma_{rr}^L(r,\phi)$ are the stresses in polar coordinates along the boundary of the hole (functions of ϕ).

The stresses in the Cartesian coordinates σ_{11}^C and σ_{22}^C at the center of the hole can be found from the solution set of kinematic variables v defined as (25) and the constitutive formulas (15)-(24).

The stresses in polar coordinates $\sigma_{\phi\phi}^L(r,\phi)$, $\sigma_{rr}^L(r,\phi)$ can be found from the stress tensor σ_{ij} in Cartesian coordinates by the following transformation:

$$\sigma_{\phi\phi} = \sigma_{11}\cos^2(\phi) + \sigma_{22}\sin^2(\phi) + (\sigma_{12} + \sigma_{21})\sin(\phi)\cos(\phi)$$

$$\sigma_{rr} = \sigma_{22}\cos^2(\phi) + \sigma_{11}\sin^2(\phi) - (\sigma_{12} + \sigma_{21})\sin(\phi)\cos(\phi)$$

Once we find J_1 and J_2, the direction of the force acting on the cavity induced by the dislocation can be calculated as follows:

$$\frac{dx_1}{dx_2} = \frac{J_1}{J_2}$$

We will model the dislocation using the two-dimensional Dirac delta function $\delta(\xi)$ being non-zero at the point of dislocation. The numerical simulation of the Dirac delta function is proposed to be done by the function (27). By shrinking the hole around the dislocation and applying the boundary conditions, we will simulate the dislocation as a limiting case of these domains. In the presence of an additional cavity this will result in a residual force, which can be calculated from the vector of solutions for kinematic variables v.

We will calculate the vector of solutions for kinematic variables v by solving

the elliptic system of partial differential Equation (26) applying the Finite Element Method developed in [17].

In our computations we consider the plates made of polyurethane foam. The polyurethane foam is known to behave as Cosserat material with the values of the technical elastic parameters presented in [24]:

$$E = 299.5 \text{ MPa},$$

$$\nu = 0.44,$$

$$l_t = 0.62 \text{ mm},$$

$$l_b = 0.327 \text{ mm},$$

$$N^2 = 0.04.$$

Taking into account that the ratio β/γ is equal to 1 for bending [24], these values of the technical constants correspond to the following values of the Lamé parameters and the Cosserat Elasticity parameters:

$$\lambda = 762.616 \text{ MPa},$$

$$\mu = 103.993 \text{ MPa},$$

$$\alpha = 4.333 \text{ MPa},$$

$$\beta = 39.975 \text{ MPa},$$

$$\gamma = 39.975 \text{ MPa},$$

$$\varepsilon = 4.505 \text{ MPa}.$$

We consider a plate 10 × 10 with its points represented on the coordinate plane by the Descartes product of the segments: $[-7,3]\times[-5,5]$. Let $h = 0.3$ be the thickness of the plate and the dislocation located at the point $(-3,2)$.

Let $G = G_1 \cup G_2$ be the external boundary of the plate:

$$G_1 = \{(x_1, x_2) : x_1 \in \{0, a\}, x_2 \in [0, a]\}$$

$$G_2 = \{(x_1, x_2) : x_2 \in \{0, a\}, x_1 \in [0, a]\}$$

and the following hard simply supported boundary conditions [19]:

$$G_1 : W = 0, W^* = 0, \Psi_2 = 0,$$

$$G_1 : \Omega_1^0 = 0, \hat{\Omega}_1^0 = 0, \Omega_3 = 0,$$

$$G_1 : \frac{\partial \Psi_1}{\partial n} = 0, \frac{\partial \Omega_2^0}{\partial n} = 0, \frac{\partial \hat{\Omega}_2^0}{\partial n} = 0;$$

$$G_2 : W = 0, W^* = 0, \Psi_1 = 0,$$

$$G_2 : \Omega_2^0 = 0, \hat{\Omega}_2^0 = 0, \Omega_3 = 0,$$

$$G_2 : \frac{\partial \Psi_2}{\partial n} = 0, \frac{\partial \Omega_1^0}{\partial n} = 0, \frac{\partial \hat{\Omega}_1^0}{\partial n} = 0.$$

The presence of the dislocation in the plate creates a stress field. This stress field can be calculated by following the procedure:

- Step 1: solve the parametric system of nine partial differential equations (26)

using the Finite Element Method developed in [17] and obtain the vector of kinematic variables (25).

- Step 2: substitute the values of the kinematic variables (25) into the constitutive formulas for the Cosserat Plate (15)-(24) and obtain the values of the two-dimensional components of stress and couple stress.

The results of the stress field σ_{11} around the dislocation in the Cosserat plate made of polyurethane foam are given in the Figure 1 & Figure 2.

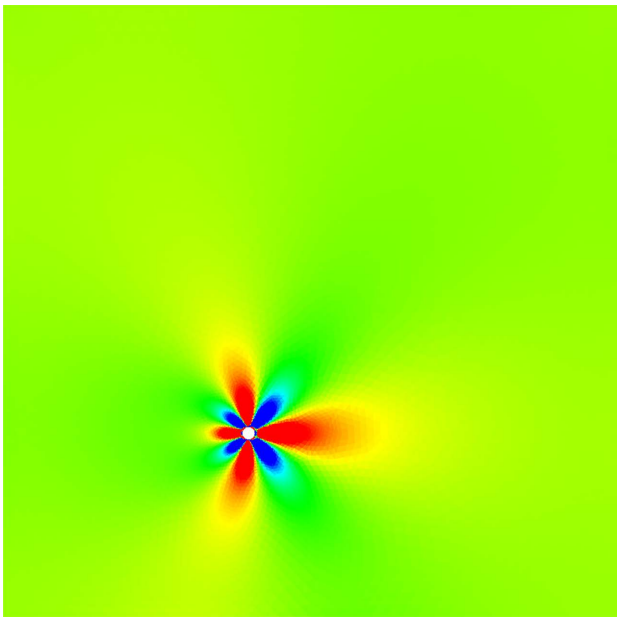

Figure 1. Distribution of the large values of σ_{11} stress component (the top 10% of the magnitude) around the dislocation in the Cosserat plate made of polyurethane foam.

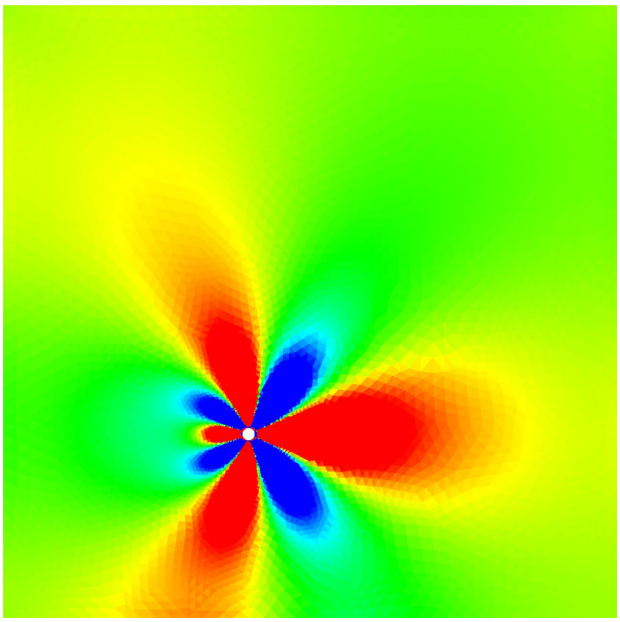

Figure 2. Distribution of the σ_{11} stress component around the dislocation in the Cosserat plate made of polyurethane foam.

Let us now add a cavity to the Cosserat plate and place it in the origin $(0,0)$ (see Figure 3). The stress fields in the Cosserat plate induce the force that acts on the cavity. The direction of the force can be obtained by the comparison of the values J_1 and J_2. The direction of the force acting on the hole is given in the Figure 4. If instead of the hole there was a crack, the direction of the residual

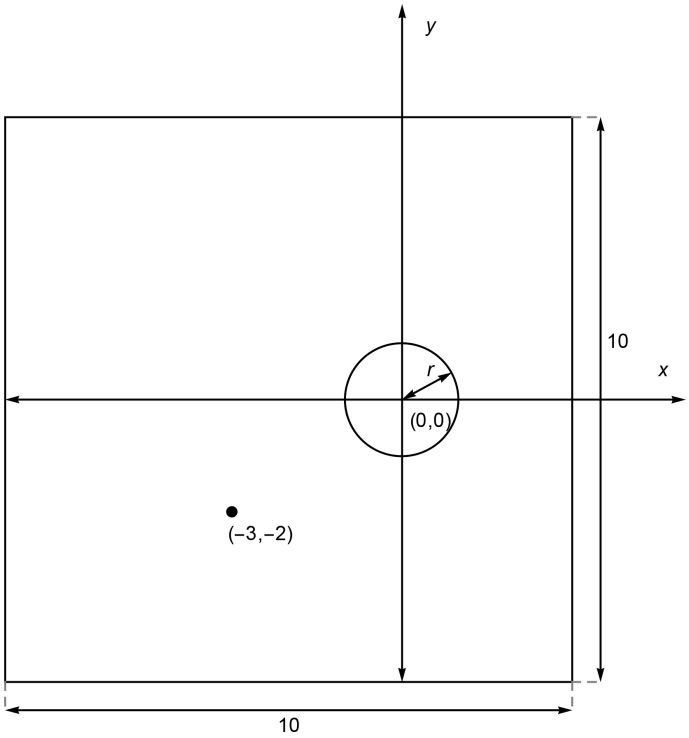

Figure 3. Perforated Cosserat plate of size 10 × 10 with the dislocation located at the point $(-3,-2)$.

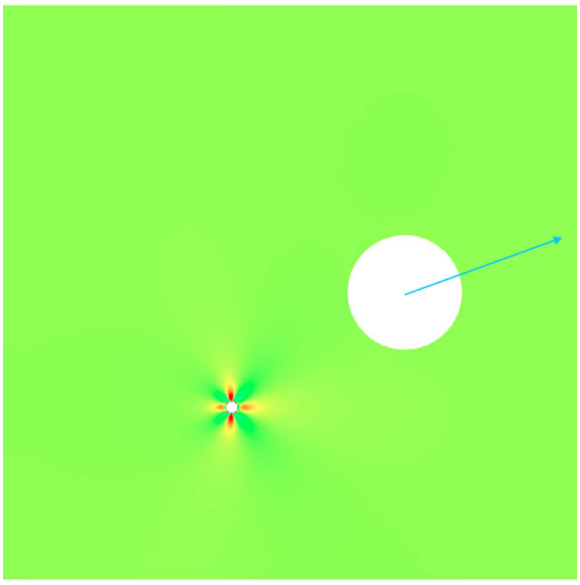

Figure 4. Direction of the force acting on the cavity in the Cosserat plate made of polyurethane foam ($J_1/J_2 = 2.47$).

force would show the trajectory of the propagation of the crack.

4. Conclusion

In this article, we presented the numerical modeling of the dislocations in the Cosserat plates based on the Cosserat Plates Theory. We modeled the dislocation by a sequence of domains that converge to the point of the dislocation and by a residual force distributed around that point. The Finite Element computations show that the presence of dislocations in a Cosserat plate will result in a stress field that will act on the cavities. We calculated the direction of the residual force acting on the cavity, which in the case of a crack, will show the trajectory of its propagation. In our future work, we plan to consider the modeling of dislocation in the framework of Cosserat Thermoelasticity.

Conflicts of Interest

The authors declare no conflicts of interest regarding the publication of this paper.

References

[1] Merkel, A., Tournat, V. and Gusev, V. (2011) Experimental Evidence of Rotational Elastic Waves in Granular Phononic Crystals. *Physical Review Letters*, **107**, Article ID: 225502. https://doi.org/10.1103/PhysRevLett.107.225502

[2] Gerstle, W., Sau, N. and Aguilera, E. (2007) Micropolar Peridynamic Constitutive Model for Concrete. 12-17.

[3] Kumar, R. (2000) Wave Propagation in Micropolar Viscoelastic Generalized Thermoelastic Solid. *International Journal of Engineering Science*, **38**, 1377-1395. https://doi.org/10.1016/S0020-7225(99)00057-9

[4] Anderson, W., Lakes, R. and Smith, M. (1995) Holographic Evaluation of Warp in the Torsion of a Bar of Cellular Solid. *Cellular Polymers*, **14**, 1-13.

[5] Lakes, R. (1986) Experimental Microelasticity of Two Porous Solids. *International Journal of Solid Structures*, **22**, 55-63. https://doi.org/10.1016/0020-7683(86)90103-4

[6] Gauthier, R. and Jahsman, W. (1975) A Quest for Micropolar Elastic Constants. *Journal of Applied Mechanics*, **42**, 369-374. https://doi.org/10.1115/1.3423583

[7] Cosserat, E. and Cosserat, F. (1909) Theory of Deformable Bodies. A. Hermann et Fils, Paris.

[8] Green, A. and Naghdi, P. (1966) The Linear Theory of an Elastic Cosserat Plate. *Mathematical Proceedings of the Cambridge Philosophical Society*, **63**, 537-550. https://doi.org/10.1017/S0305004100041487

[9] Eringen, A. (1967) Theory of Micropolar Plates. *Journal of Applied Mathematics and Physics*, **18**, 12-31. https://doi.org/10.1007/BF01593891

[10] Steinberg, L. (2010) Deformation of Micropolar Plates of Moderate Thickness. *International Journal Applied Mathematics and Mechanics*, **6**, 1-24.

[11] Kvasov, R. and Steinberg, L. (2011) Numerical Modeling of Bending of Cosserat Elastic Plates. *Proceedings of the* 5*th Computing Alliance of Hispanic-Serving Institutions Annual Meeting*, San Juan, March 27-29, 2011, 67-70.

[12] Steinberg, L. and Kvasov, R. (2013) Enhanced Mathematical Model for Cosserat Plate Bending. *Thin-Walled Structures*, **63**, 51-62. https://doi.org/10.1016/j.tws.2012.10.003

[13] Reissner, E. (1944) On the Theory of Elastic Plates. *Journal of Mathematics and Physics*, **23**, 184-191. https://doi.org/10.1002/sapm1944231184

[14] Reissner, E. (1945) The Effect of Transverse Shear Deformation on the Bending of Elastic Plates. *Journal of Applied Mechanics*, **12**, 69-77. https://doi.org/10.1115/1.4009435

[15] Kvasov, R. and Steinberg, L. (2013) Numerical Modeling of Bending of Micropolar Plates. *Thin-Walled Structures*, **69**, 67-78. https://doi.org/10.1016/j.tws.2013.04.001

[16] Steinberg, L. and Kvasov, R. (2015) Analytical Modeling of Vibration of Micropolar Plates. *Applied Mathematics*, **6**, 817-836. https://doi.org/10.4236/am.2015.65077

[17] Kvasov, R. and Steinberg, L. (2017) Modeling of Size Effects in Bending of Perforated Cosserat Plates. *Modelling and Simulation in Engineering*, **2017**, Article ID: 5246197. https://doi.org/10.1155/2017/5246197

[18] Steinberg, L. and Kvasov, R. (2019) Distinctive Characteristics of Cosserat Plate Free Vibrations. *Dynamical Systems Theory*, **6**, 817-836. https://doi.org/10.5772/intechopen.87044

[19] Steinberg, L. and Kvasov, R. (2022) Cosserat Plate Theory. CRC Press, Boca Raton. https://doi.org/10.1201/9781003190264

[20] Kienzler, R. and Herrmann, G. (2000) Linear Elasticity with Defects. In: Kienzler, R. and Herrmann, G., Eds., *Mechanics in Material Space with Application to Defect and Fracture Mechanics*, Springer, Berlin, 95-119. https://doi.org/10.1007/978-3-642-57010-0_5

[21] Kadic, A. and Edelen, D. (1983) A Gauge Theory of Dislocations and Disclinations. Lecture Notes in Physics, Vol. 174, Springer, Berlin. https://doi.org/10.1007/3-540-11977-9

[22] Ahmad, A., *et al.* (2022) Influence of Hartmann Number on Convective Flow of Maxwell Fluid between Two Hot Parallel Plates through Porous Medium Subject to Arbitrary Shear Stress at the Boundary. *Journal of Applied Mathematics and Physics*, **10**, 160-171. https://doi.org/10.4236/jamp.2022.101012

[23] Iqbal, S., Sarwar, F. and Raza, S. (2016) Quantum Mechanical Tunneling of Dislocations: Quantization and Depinning from Peierls Barrie. *World Journal of Condensed Matter Physics*, **6**, 103-108. https://doi.org/10.4236/wjcmp.2016.62014

[24] Lakes, R. (1995) Ch. 1. Experimental Methods for Study of Cosserat Elastic Solids and Other Generalized Elastic Continua. In: Mühlhaus, H., Ed., *Continuum Models for Materials with Micro-Structure*, Wiley, Hoboken, 1-22.

Notations

x_i	Cartesian coordinates
B	Cosserat body
P	Cosserat plate
H	plate thickness
μ, λ	Lamé parameters
$\alpha, \beta, \gamma, \varepsilon$	Cosserat elasticity parameters
σ_{ji} or $\boldsymbol{\sigma}$	stress tensor
μ_{ji} or $\boldsymbol{\mu}$	couple stress tensor
γ_{ji} or $\boldsymbol{\gamma}$	strain tensor
χ_{ji} or $\boldsymbol{\chi}$	torsion tensor
u_i or $\boldsymbol{u}$	displacement vector
ϕ_i or $\boldsymbol{\phi}$	microrotation vector
b_i or $\boldsymbol{b}$	Burger's vector
w_{ij} or $\boldsymbol{w}$	distortion tensor
k_{ij} or $\boldsymbol{g}$	material stress tensor
ε_{ijk}	Levi-Civita tensor
V	Cosserat plate displacement set
η	splitting parameter
P	pressure
$M_{\alpha\beta}$	bending and twisting moments
Q_α	shear forces
$Q_\alpha^*, \hat{Q}_\alpha$	transverse shear forces
$R_\alpha^*, \hat{R}_\alpha$	Cosserat bending and twisting moments
S_α	Cosserat couple moments
Ψ_α	rotations of the middle plane around x_α axis
W, W^*	vertical deflections of the middle plate
$\Omega_\alpha^*, \hat{\Omega}_\alpha$	microrotations in the middle plate around x_α axis
Ω_3	rate of change of the microrotation